Microfluid Nanofluid
DOI 10.1007/s10404-011-0787-4

RESEARCH PAPER

Time-resolved dynamics of laser-induced micro-jets from thin liquid films

Matthew S. Brown · Nicholas T. Kattamis · Craig B. Arnold

Received: 17 December 2010 / Accepted: 10 March 2011

Abstract Laser-induced forward transfer (LIFT) is a high-resolution direct-write technique, which can print a wide range of liquid materials without a nozzle. In this process, a pulsed laser initiates the expulsion of a high-velocity micro-jet of fluid from a thin donor film. LIFT involves a novel regime for impulsively driven free-surface jetting in that viscous forces developed in the thin film become relevant within the jet lifetime. In this work, time-resolved microscopy is used to study the dynamics of the laser-induced ejection process. We consider the influence of thin metal and thick polymer laser-absorbing layers on the flow actuation mechanism and resulting jet dynamics. Both films exhibit a mechanism in which flow is driven by the rapid expansion of a gas bubble within the liquid film. We present high-resolution images of the transient gas cavities, the resulting ejection of high aspect ratio external jets, as well as the first images of re-entrant jets formed during LIFT. These observations are interpreted in the context of similar work on cavitation bubble formation near free surfaces and rigid interfaces. Additionally, by increasing the laser beam size used on the polymer absorbing layer, we observe a transition to an alternate mechanism for jet formation, which is driven by the rapid expansion of a blister on the polymer surface. We compare the dynamics of these blister-actuated jets to those of the gas-actuated mechanism. Finally, we analyze these results in the context of printing sensitive ink materials.

Electronic supplementary material The online version of this article (doi:10.1007/s10404-011-0787-4) contains supplementary material, which is available to authorized users.

M. S. Brown · N. T. Kattamis · C. B. Arnold (✉)
Department of Mechanical and Aerospace Engineering, Princeton University, Princeton, NJ 08544, USA
e-mail: cbarnold@princeton.edu

Keywords Laser-induced forward transfer · Cavitation · Re-entrant jet · Printing

1 Introduction

Nozzle-based printing techniques are important tools for the rapid fabrication of device prototypes and are currently being investigated as environmentally friendly, economical alternatives to traditional large-volume manufacturing processes (Calvert 2001; Hon et al. 2008; Singh et al. 2010). However, the reliability of these methods and the range of ink materials that can be printed are ultimately limited by the presence of a nozzle, which can be subject to clogging and material compatibility issues. Alternatively, laser-induced forward transfer (LIFT) is an emerging high-resolution printing technique, which can deposit a wide range of structural and functional materials without the use of a nozzle (Piqué et al. 1999; Piqué et al. 2006; Kyrkis et al. 2006; Arnold et al. 2007). In this process, a pulsed laser initiates the ejection of a small volume of ink from a thin liquid donor film (1–100 μm), which is supported by a laser-transparent glass substrate, onto a parallel receiver substrate held at a distance (10–1000 μm). Under appropriate conditions, transfer is mediated by a high-velocity micro-jet, which achieves a high aspect ratio before detaching from the donor film (Young et al. 2002; Duocastella et al. 2008; Brown et al. 2010).

Most studies on rapidly accelerated free-surface jets have focused on their formation from the surface of a bulk fluid domain (Blake and Gibson 1987; Zeff et al. 2000; Duchemin et al. 2002; Antkowiak et al. 2007; Gekle et al. 2009). However, LIFT involves a relatively unstudied configuration in that the propagating jet draws from a thin film, in which viscous forces become relevant. For example, considering a typical 10-μm thick donor film of ink

Published online: 27 March 2011

with kinematic viscosity $v = 10$ cSt, a viscous boundary layer will grow in thickness as $\sqrt{v\tau}$ and span the film within $\tau \approx 10$ μs, which is a fraction of a typical jet lifetime. Flow within the film, which is initially dominated by inertial forces, becomes increasingly influenced by viscous forces during the later stages of jet propagation. The effect of this interplay of inertial and viscous forces on the dynamics of the jet and the onset of its pinch-off from the film remains an open question. Therefore, the LIFT experiment provides a useful platform in which to probe the fluid dynamics of this novel and technologically relevant regime of free-surface jetting from thin films.

The mechanism by which the absorbed laser energy actuates flow during LIFT is largely influenced by the donor film properties and the presence of an intermediary laser-absorbing layer. For example, transfers initiated by direct absorption within the ink (Young et al. 2002; Lewis et al. 2006) or within a metal-film absorbing layer (Barron et al. 2005; Duocastella et al. 2008) are generally attributed to the formation of a rapidly expanding vapor cavity. This proposed mechanism parallels similar behavior of cavitation bubbles near the surface of a bulk fluid. Studies demonstrate that a cavitation bubble can produce an external free-surface spike as well as an internal re-entrant jet and that these structures become narrower and more prominent with decreasing non-dimensional standoff distance $\gamma = h/R_m$, which relates the cavity's initial depth beneath the surface h to its maximum radius R_m (Blake and Gibson 1987; Robinson et al. 2001; Pearson et al. 2004). However, these studies draw upon a limited range of experimental results, which consider much larger bubbles ($R_m > 1$ mm) and at greater standoff distances ($\gamma > 0.5$) than those expected during LIFT. In addition to this vapor-cavity-driven mechanism, transfers have also been demonstrated using a polymer-film absorbing layer that produces a rapidly expanding blister (Brown et al. 2010). Further study into the nature of these transfer mechanisms is required to better understand the stresses placed on the ink and motivate ways to mitigate damage to sensitive donor materials.

In this work, we use time-resolved microscopy to study the laser-induced formation and propagation of high-speed micro-jets from thin films of a model ink system. We compare the dynamics of jets initiated with a polyimide absorbing layer to those from the more commonly studied metal-film absorbing layer, which provides a reference case. Using the minimum laser spot size provided by our experimental setup (2.5 μm), we identify an ejection mechanism from the polyimide layer in which the film ruptures and releases a bubble of hot gas into the ink (Fig. 1c). The resulting ejection dynamics are similar to those from a titanium absorbing layer, in which flow is predominantly driven by a bubble of vaporized ink

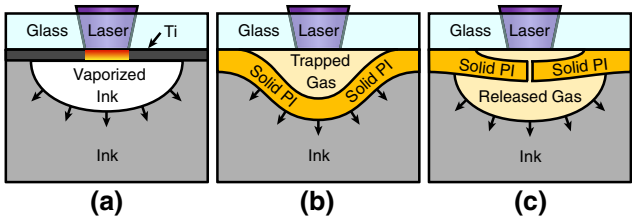

Fig. 1 (Color online) Mechanisms for laser-induced actuation of flow within the ink film. **a** Laser absorption within a titanium (Ti) film results in vaporization of the adjacent ink, producing a high-pressure vapor cavity. **b** Laser absorption within a polyimide (PI) film produces a rapidly expanding, sealed blister. **c** Above a threshold laser energy, the polyimide film ruptures and releases high-pressure gases

(Fig. 1a). The gas-actuated ejections from both films involve the formation of a rapidly expanding gas cavity, which becomes large ($R_m \approx 45$ μm) relative to the liquid film thickness ($\gamma \approx 0.1$). This produces a high aspect ratio free-surface jet, which propagates away from the transient cavity. We present the first direct evidence of re-entrant jet formation within the cavity during LIFT. However, the re-entrant jets are highly suppressed relative to inviscid flow predictions. Using a larger beam size (10 μm) on the polyimide layer, we demonstrate a transition to a blister-actuated ejection mechanism (Fig. 1b), which results in jetting dynamics that are characteristically different than those from the gas-actuated regime. Finally, we highlight the practical differences between the ejection mechanisms with respect to printing of sensitive ink materials.

2 Experimental methods

Donor substrates are prepared by first depositing a sacrificial laser-absorbing layer onto standard glass microscope slides. To investigate the effects of the absorbing-layer material on the dynamics of ink ejection, two different sets of donor substrates are produced. One set is coated with 50 nm of titanium by e-beam evaporation. The other set is prepared, as detailed in Brown et al. (2010), by spin coating polyimide resin (HD Microsystems PI2525) onto the glass and baking to produce a 7-μm thick film, as measured by confocal microscopy. The donor liquid used in these experiments is an aqueous solution of glycerol (50% v/v) with Triton X-100 surfactant (1.4% v/v), a model system similar to that used in related studies (Colina et al. 2006; Duocastella et al. 2008). The solution has a surface tension of 32 mN/m, a viscosity of 7.5 mPa s, and a density of 1.123 g/cm^3. The liquid is spread into a thin film ($\sim$5 μm thick) onto the laser-absorbing layer using a Mayer rod.

Donor assemblies are placed in a standard LIFT configuration (Arnold et al. 2007) without a receiver substrate

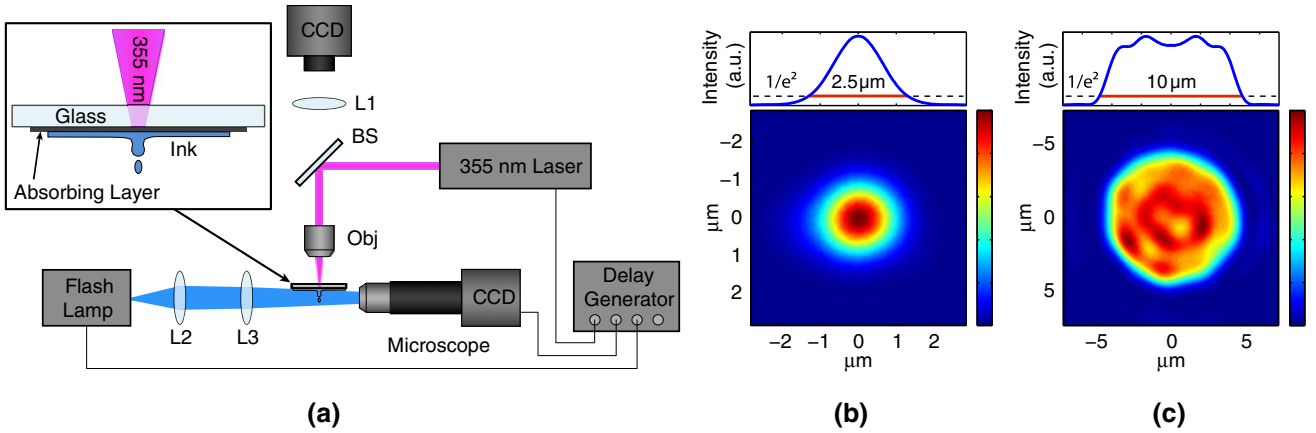

Fig. 2 (Color online) **a** Diagram of the LIFT-imaging apparatus. A UV laser is focused through an objective (Obj) onto the laser-absorbing layer of the donor assembly (*inset*). A *top-view* image of the sample, acquired through Obj and a beam splitter (BS), is focused onto a CCD camera by a tube lens (L1). A flash lamp, collector lens (L2), and condenser lens (L3) provide a pulse of uniform illumination to the ejected material, which is imaged from the side by a microscope and CCD camera. **b** Beam-profiler images of the 2.5-μm Gaussian and **c** 10-μm top-hat beam as well as profiles of the average intensity versus radius

(Fig. 2a). Liquid ejection is initiated by focusing a pulse from a frequency-tripled Nd:YVO_4 laser (Coherent AVIA, $\lambda = 355$ nm, $\tau = 20$ ns) through the glass slide into the absorbing layer (inset of Fig. 2a) using a 15× UV laser objective (numerical aperture of 0.32). A Gaussian profile with a 2.5-μm full width at $1/e^2$ maximum is achieved on the absorbing layer by positioning it in the focal plane of the objective. To assist in substrate positioning, a visible image of this plane is also acquired through the laser objective using a secondary tube lens and a charge-coupled device (CCD) camera. Additionally, 5 and 10-μm top-hat beam profiles are created by projecting the reduced image of a pinhole onto the donor film (see Brown et al. (2010) for more details). A beam profiler is used to fine-tune the system's focus and verify the dimensions of the beam in the sample plane (Fig. 2b, c; more details in Online Resource 1). To account for absorption and reflection losses from the donor-support glass, laser pulse energy is measured through an uncoated glass slide with an energy meter.

Time-resolved images of the ejected fluid are acquired from the side using a stroboscopic imaging system (Fig. 2a). Jet formation is initiated by a single pulse of the UV laser beam. After a delay, a single image is captured with a microscope (InfiniTube with a Mitutoyo 50× Long-WD Objective) and a CCD camera (SPOT Insight IN1820) by strobing a $\tau = 25$ ns plasma discharge lamp (HSPS Nanolite). The CCD integration time (500 μs) extends over the entire ejection process, but the image is only exposed over the duration of the strobe pulse. Strobe timing is set with a digital delay generator (SRS DG535), and the image exposure delay is calibrated by measuring both the laser and strobe signals with a photodiode and an oscilloscope. The donor assembly is translated to an unused location between each laser shot. Twenty to thirty liquid ejections are imaged at each exposure delay, which is successively increased to capture a continuous progression of the entire jetting process. The images are processed with a custom MATLAB program to extract the dimensions of the observed fluid structures.

3 Results and discussion

3.1 Gas-actuated liquid ejection

Time-resolved images of jets expelled from a 5-μm liquid donor film using a 50-nm titanium laser-absorbing layer are shown in Fig. 3. Fluid motion is initiated by focusing a 1.6-μJ laser pulse into the titanium layer to a 2.5-μm Gaussian spot. The applied laser energy corresponds to the threshold at which the fluid jets produced are sufficiently energetic to consistently detach from the liquid film. This threshold energy regime is particularly relevant for high-resolution printing as it produces the smallest transferred volumes (Colina et al. 2006; Serra et al. 2006). The image sequence depicts jetting dynamics that are consistent with previous studies (Duocastella et al. 2008). However, these images provide higher resolution detail of the fluid near the interface, allowing analysis of the initial cavity expansion and subsequent collapse dynamics.

Irradiation of the titanium film results in rapid heating and explosive boiling of the adjacent liquid, producing a high-pressure vapor cavity, which expands and drives flow in the remaining film (Fig. 1a). The inflating cavity rapidly displaces the free surface of the liquid (initially 200 m/s) and results in a distended protrusion, which broadens and

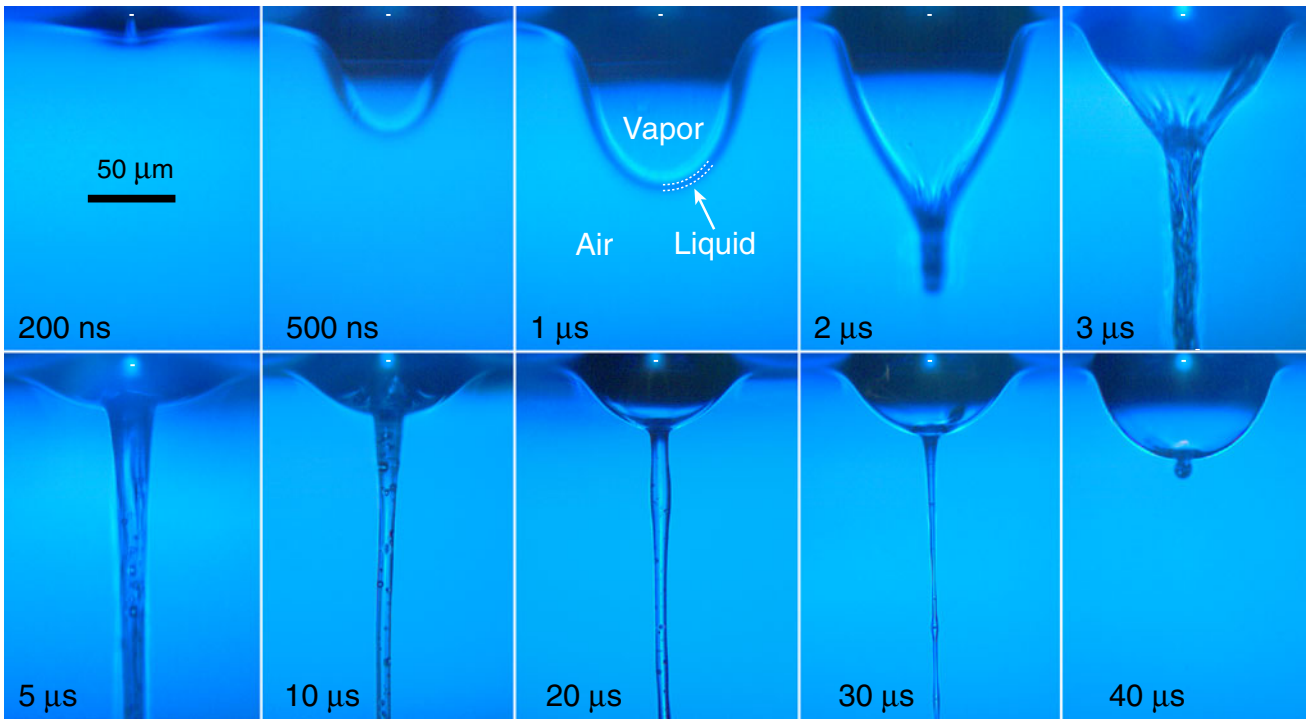

Fig. 3 (Color online) Time-resolved images of liquid ejection into the ambient air using a 50-nm titanium absorbing layer. A 1.6-µJ laser pulse is focused into the titanium film to a spot size of 2.5 µm (indicated by a white marker), initiating liquid ejection from an adjacent 5-µm film. Laser-induced plasma generated during the 20-ns laser pulse is captured even in images strobed at much later times because the CCD shutter remains open during the entire transfer. The vertical field of view of each image is ~200 µm

propagates downward with time (Fig. 4a, b). A several-micron-thick dark rim surrounds the protrusion and approximately indicates the liquid layer that encloses the vapor pocket. This is consistent with the initial 5-µm thickness of the liquid donor film, which becomes thinned by its expansion. As the cavity expands and the enclosed vapor cools, the internal pressure continues to drop until it can no longer overcome the external atmospheric pressure and surface tension of the liquid. The cavity reaches a maximum size by 1–2 µs and then begins to collapse. However, the momentum developed during the initial expansion causes the rapidly moving liquid film to continue downward and funnel into a thin jet, which develops at the tip of the protrusion. By 3 µs, the cavity has partially collapsed, but the jet continues to propagate downward, pulling liquid through the thin film of its bubble-like base. Although the jet front exceeds the field of view, similar studies observe it to proceed with approximately constant velocity and attain lengths on the order of a millimeter before breaking up (Duocastella et al. 2009). By 5 µs, the vapor cavity has fully collapsed. However, it then rebounds and undergoes a secondary expansion (Akhatov et al. 2001), which is enhanced by the tension from the continually drawing jet. It is possible that air becomes entrained by the flow and enters the cavity during this rebound phase. As the jet continues to propagate, the diameter near its base

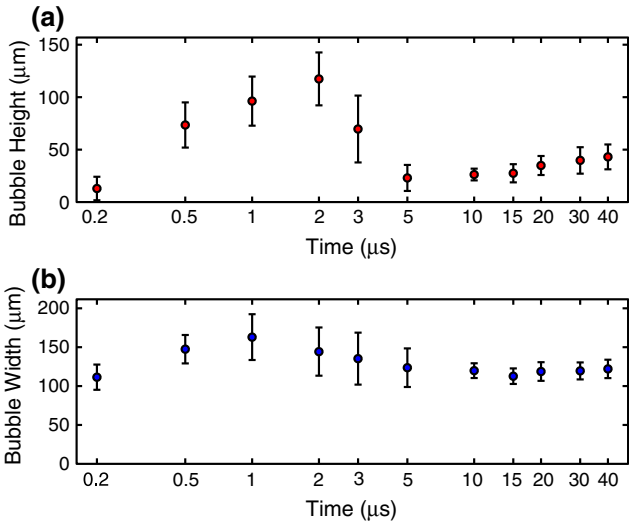

Fig. 4 (Color online) Measurements extracted from images of laser-induced vapor bubbles produced for the conditions of Fig. 3. Error bars indicate ±1 standard deviation in the values. **a** Bubble height, which is defined as the vertical displacement of the liquid film relative to the surrounding undisturbed surface, is plotted as a function of logarithmic time. After a jet has formed, bubble height is measured to the intersection of the jet with its bubble-like base. **b** Bubble width is measured in the plane of the original film surface

decreases from 15–25 µm at 5 µs to 3–5 µm at 30 µs. Eventually, the jet pinches off from its bubble-like base, which subsequently bursts.

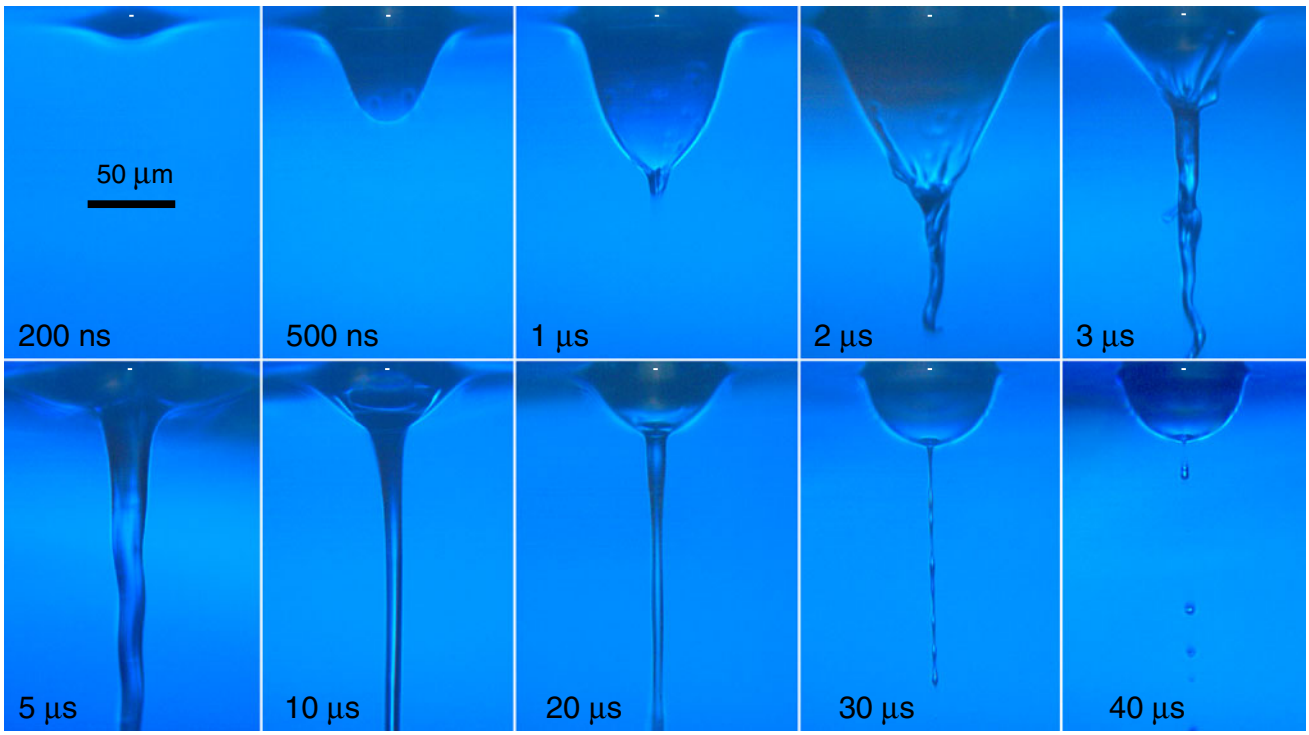

Fig. 5 (Color online) Time-resolved images of liquid ejection into the ambient air using a 7-µm polyimide absorbing layer. A 1.0-µJ laser pulse is focused into the polyimide film to a spot size of 2.5 µm (indicated by a white marker), initiating liquid ejection from an adjacent 5-µm film. The vertical field of view of each image is ~200 µm

A similar sequence of images is shown in Fig. 5 of fluid jets ejected using a 7-µm polyimide absorbing layer. Once again, the laser is focused to a 2.5-µm Gaussian spot with a pulse energy (1.0 µJ) that corresponds to the fluid ejection threshold. Despite the differences in thickness and material properties between the absorbing layers used in Figs. 3 and 5, the resulting ejection dynamics appear almost identical, both in the dimensions and temporal evolution of the features formed (Fig. 6a, b). This indicates a similar mechanism for jet formation.

The polyimide film absorbs the laser within a thin layer near the glass interface, resulting in a confined pocket of high-temperature, high-pressure decomposition products. Below a critical laser energy, these expanding gases remain sealed within the polyimide film, which is deformed into a rapidly inflating blister (Brown et al. 2010). However, for the conditions of Fig. 5, SEM images of the polyimide film indicate that the observed ejection threshold coincides with the threshold for blister rupture. Therefore, the fluid ejection is predominantly propelled by the release of hot gases from the ruptured film (Fig. 1c). This results in similar dynamics to those previously described for Fig. 3.

The image sequences in Figs. 3 and 5 are both examples in which jets are initiated by the violent expansion and

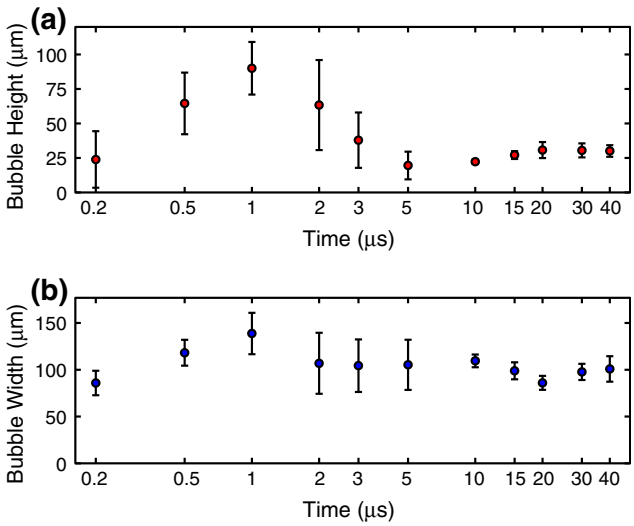

Fig. 6 (Color online) Measurements extracted from images of laser-induced vapor bubbles produced for the conditions of Fig. 5. Error bars indicate ±1 standard deviation in the values. **a** Bubble height, which is defined as the vertical displacement of the liquid film relative to the surrounding undisturbed surface, is plotted as a function of logarithmic time. After a jet has formed, bubble height is measured to the intersection of the jet with its bubble-like base. **b** Bubble width is measured in the plane of the original film surface

collapse of a gas bubble within the liquid film. We can analyze these observations in the context of similar studies on the dynamics of cavitation bubbles that form near an interface. When a cavitation bubble forms in proximity to the free surface of a bulk fluid, its expansion is highly asymmetric, favoring displacement of the fluid near the surface over that within the semi-infinite bulk (Blake and Gibson 1987; Robinson et al. 2001; Pearson et al. 2004). Inviscid flow simulations show that as this expansion slows, a high-pressure stagnation point develops between the bubble and the surface. This drives the formation of a propagating free-surface spike as well as a counter-propagating re-entrant jet, which intersects the collapsing bubble and impinges on its opposite wall. The studies show that these structures becomes sharper and more prominent with decreasing non-dimensional standoff distance $\gamma = h/R_m$.[1] However, this trend is based on results from a limited range of R_m and γ, in which viscous and surface forces are not likely to be important (Blake and Gibson 1987; Robinson et al. 2001; Pearson et al. 2004).

The gas cavities produced in Figs. 3 and 5 are about 25 times smaller and 5 times closer to the surface ($R_m \approx 45$ μm and $\gamma \approx 0.1$ for both sequences) than those previously studied (Blake and Gibson 1987; Robinson et al. 2001; Pearson et al. 2004). The formation of bubbles with such small γ is possible because surface tension suppresses instabilities at the cavity wall and prevents bursting. The criterion for bubble bursting is often expressed in terms of a critical Weber number $We_c = \rho v^2 l/\sigma$, where ρ is the liquid density and σ is the surface tension. This demonstrates that the maximum stable characteristic velocity v increases as the system length scale l is reduced. Thus, the process results in a highly elongated cavity expansion and a high aspect ratio external jet, which is consistent with the γ-scaling trend for cavitation bubbles near the surface of a bulk fluid.

Additionally, one would expect a prominent re-entrant jet to form in this system. In the context of LIFT, re-entrant jets have been speculated (Duocastella et al. 2009) and are relevant as a source of high temperature and pressure, which may cause damage to sensitive inks or the rigid support. Re-entrant jet formation during cavitation bubble collapse near a rigid boundary has long been studied with the interest of better understanding the mechanism for cavitation-induced damage (Benjamin and Ellis 1966; Plesset and Chapman 1971; Blake and Gibson 1987; Philipp and Lauterborn 1998; Brujan et al. 2001). Studies show that cavity collapse near a rigid boundary can result in a re-entrant jet in the direction of the boundary. Therefore, since LIFT involves the composite case of a collapsing cavity in proximity to both a free surface and a rigid boundary, we would expect a pronounced and intense re-entrant jet. This is supported by recent numerical simulations that demonstrate re-entrant jet formation during LIFT, although without considering viscous or surface forces (Mézel et al. 2009). However, none of the images acquired for the conditions of Fig. 3 or 5 exhibit any evidence of a re-entrant jet.

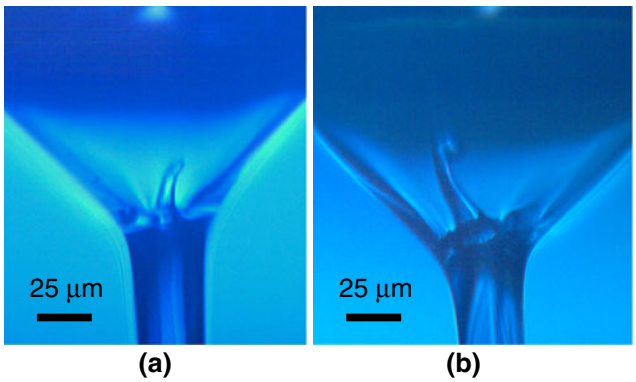

Fig. 7 (Color online) Close-up images acquired at 5 μs of gas cavities formed during the ejection of liquid from a 5-μm film using **a** titanium (11.8 μJ) and **b** polyimide (7.3 μJ) absorbing layers with a 2.5-μm beam. Internal re-entrant jets (directed upwards) are clearly visible within the gas cavity

The absence of re-entrant jets in these images can be attributed to the significance of viscous forces and surface tension, which cannot be neglected in the case of LIFT. The assumption of inviscid flow is typically justified by demonstrating that the calculated boundary layer thickness remains small relative to the system dimensions. However, in our case, the boundary layer grows to span the 5-μm film thickness within ~3 μs. Therefore, viscous forces become relevant within the timescale of the cavity collapse and act to suppress the re-entrant jet. We can begin to see evidence of weakly formed re-entrant jets in ejections from both absorbing layers using higher laser energies (~7 times the ejection threshold), which produce larger cavities ($R_m > 70$ μm) and more energetic flow. Two of the most pronounced examples are shown in Fig. 7, in which the re-entrant jets reach a maximum size of 20–30 μm within 5 μs, before coalescing back into the liquid. Their internal propagation appears to be inhibited by shear stresses from the more dominant downward flow into the main jet (Yu et al. 1995). This is consistent with similar observations that the velocity of a re-entrant jet can be reduced or even entirely suppressed by viscous forces (Chahine and Fruman 1979; Brujan et al. 1996; Popinet and Zaleski 2002; Liu et al. 2009; Minsier et al. 2009).

3.2 Blister-actuated fluid ejection

By increasing the laser beam size used on the polyimide absorbing layer, we observe a transition in the mechanism

[1] For non-spherical cavities, R_m is the radius of a sphere with an equivalent volume.

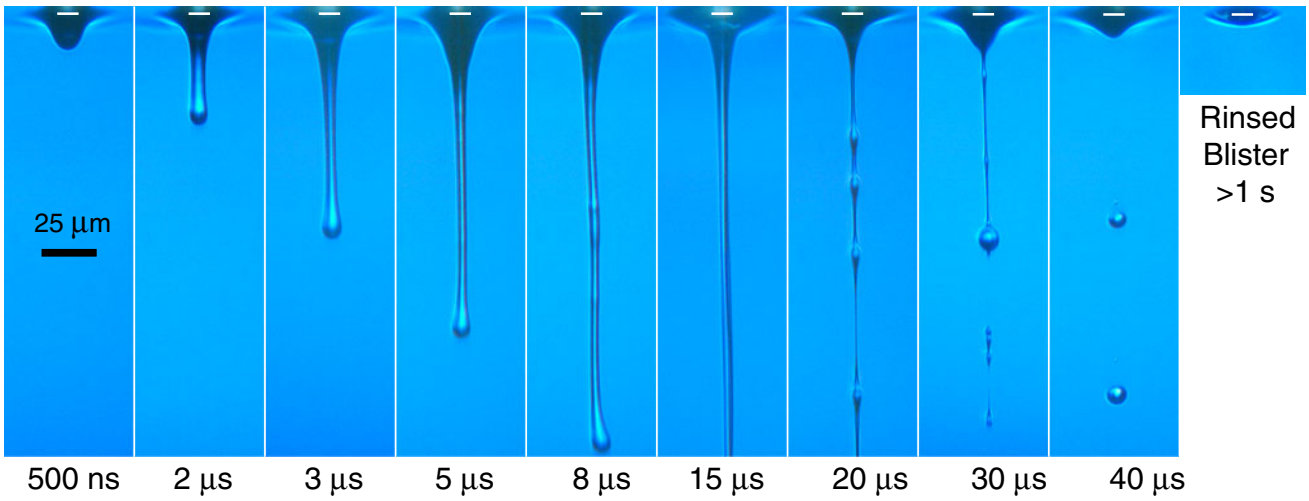

Fig. 8 (Color online) Time-resolved images of liquid jets expelled into the ambient air using a 7-µm polyimide absorbing layer. A 2.7-µJ laser pulse is focused into the polyimide film to a spot size of 10 µm (indicated by a white marker), producing a rapidly expanding, sealed blister, which initiates liquid ejection from an adjacent 5-µm film. The vertical field of view is ~200 µm. An image (>1 s) of the blister, rinsed of residual liquid, is shown for reference

driving the fluid ejection. The largest blisters produced with the 2.5-µm beam are too small to provide a sufficient impulse for fluid ejection. Instead, threshold ejections are propelled by the high-pressure gases discharged from the ruptured film. By increasing the laser beam size used, larger blisters can be formed on the polyimide film without rupture, allowing a greater impulse to the fluid (Brown et al. 2010). Results using a 5-µm beam still show that film rupture is required for ejection. Yet, with a 10-µm incident beam, sufficiently large blisters can be produced such that a transition from a gas-actuated ejection mechanism to a purely blister-actuated mechanism occurs at the ejection threshold.

A time-resolved sequence of jets expelled by blisters formed on a 7-µm polyimide absorbing layer is shown in Fig. 8. The fluid motion is initiated by focusing a 2.7-µJ laser pulse into the polyimide film to a 10-µm top-hat spot. This applied laser energy corresponds to the threshold at which the fluid jets consistently detach from the liquid film. SEM images verify that the polyimide film does not rupture and the hot gases remain trapped within the blister, which, due to the low thermal diffusivity of the polyimide ($\alpha = 9.7 \times 10^{-8}$ m^2/s),[2] prevents significant thermal interaction with the adjacent liquid. Additionally, the images of Fig. 8 do not show any indication of cavitation within the liquid. Therefore, fluid motion is solely driven by the deforming blister's exterior surface (Fig. 1b), resulting in ejection dynamics that are characteristically different from those of Fig. 5.

The blister expands to a maximum size (6.3 ± 0.4 µm high by 35.5 ± 0.6 µm wide) within 100 ns. This provides an impulse to the adjacent liquid over the spatial extent of the blister. The corresponding region of high-momentum fluid develops into a free-surface jet, which initially propagates with a constant jet-front velocity of ~25 m/s before exceeding the field of view. This initial velocity is about 5 times lower than the gas-actuated jets of Fig. 5. Continued propagation is maintained by the momentum of the jet, which pulls additional fluid from the surrounding film. A boundary layer develops and spans the film thickness within ~3 µs. Therefore, viscous forces become relevant early in the jetting process. Additionally, the influence of surface tension is apparent in the rounded teardrop tip of the jet and the imposed curvature at its base. As the jet continues to extend from the film, the diameter at its base increases slightly from 40 to 45 µm (Fig. 9a), while a local minimum in diameter (i.e., a neck) develops near the jet midpoint and decreases with increasing jet length (Fig. 9b). During the later stages of jet propagation, a bead-like perturbation develops and grows due to the Rayleigh–Plateau instability (Eggers 1997), which causes the jet to break up into spherical droplets.

3.3 Comparison of ejection mechanisms

Despite the similarities in the dynamics of the gas-actuated ejections (Figs. 3, 5), there are practical differences in transferring material with the two absorbing layers, which become relevant when considering functional or sensitive inks (Kattamis et al. 2009). For transfers with a metal-film absorbing layer, the gas is predominantly derived from the vaporized ink. This assertion is supported by evidence that fluid transfers are possible even in cases in which the metal film remains entirely intact (Colina et al. 2006; Serra et al.

[2] Manufacturer's specification.

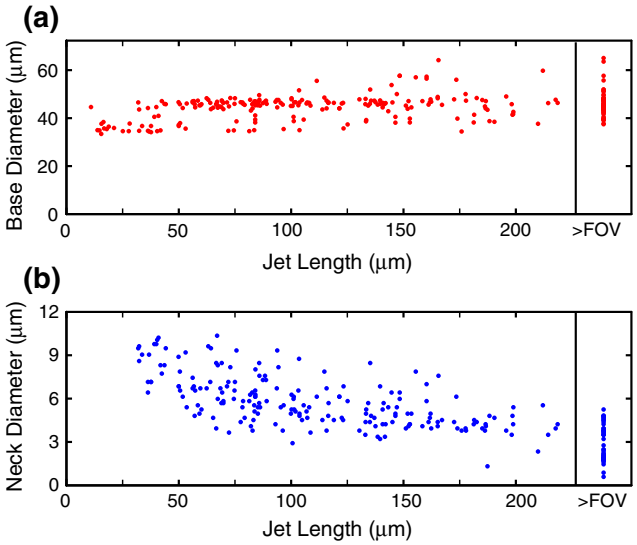

Fig. 9 (Color online) Measurements from images of blister-actuated jets produced with the conditions of Fig. 8. **a** Diameter of the jet measured at its base plotted versus jet length. Measurements from images in which the jet tip exceeds the field of view (FOV) are shown at the right. **b** Jet diameter measured at a region of local minimum (i.e., neck) plotted versus jet length. Jets shorter than ~30 μm do not exhibit a neck and are excluded from the data

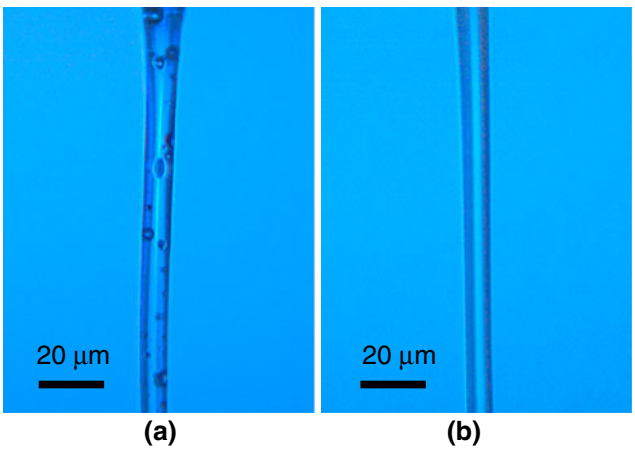

Fig. 10 (Color online) Close-up images acquired at 10 μs of jets expelled from a 5-μm liquid film using **a** titanium (1.6 μJ) and **b** polyimide (1.0 μJ) absorbing layers with a 2.5-μm beam. **a** Hot fragments of the titanium film nucleate additional micron-sized vapor bubbles, which become entrained in the jet. **b** Such bubbles are not present in the jets produced with the polyimide film

2006). In most cases, however, hot fragments of the metal film are incorporated into the ejected material, which can lead to contamination (Smausz et al. 2006), and cause pyrolytic damage to sensitive ink materials (Kattamis et al. 2009). Furthermore, these hot fragments nucleate micron-sized vapor bubbles, which become entrained within the jet (Fig. 10a), and can cause additional damage as they collapse. This type of damage is avoided in gas-actuated ejections from polyimide, which consistently lack evidence of such secondary bubbles (Fig. 10b). However, both gas-actuated transfer mechanisms (Fig. 1a, c) inherently involve the formation and collapse of a cavity, which has been shown to be a source of high temperatures and pressures (Philipp and Lauterborn 1998). Therefore, some degree of damage to the ink may be fundamentally unavoidable in these cases. In contrast, blister-actuated transfers (Fig. 1b) do not expose the ink to hot gases, and there is no evidence of cavitation within the liquid. Therefore, the blister-actuated transfer mechanism may be the optimal approach for preventing damage to sensitive inks (Kattamis et al. 2007).

4 Conclusions

In summary, this work presents new insights into the mechanisms for laser-induced formation and propagation of jets from thin liquid films using different absorbing-layer materials and laser focusing conditions. In each case, we apply a laser energy corresponding to the threshold for jet pinch-off, which is a relevant regime for high-resolution LIFT printing of delicate organic or biological material. Ejections from a polyimide absorbing layer exhibit two distinct ejection mechanisms depending on the laser beam size. With a larger laser spot (10 μm), blisters produced on the polyimide provide a sufficient impulse to expel a jet from the liquid film. These blister-actuated jets initially propagate at a constant velocity (~25 m/s) with a diameter that is comparable to the laser spot size. Due to their small dimensions and low velocity, surface tension has a noticeable influence on the jet shape. Alternatively, with a smaller laser spot (2.5 μm), the polyimide film ruptures before the blister-actuated ejection threshold is reached. Instead, jetting is due to the rapid expansion of a gas cavity released from the ruptured film. A similar mechanism occurs with a titanium absorbing layer, in which the gas cavity is predominantly derived from the vaporized liquid. Both gas-actuated mechanisms exhibit similar ejection dynamics. The expanding gas cavity rapidly displaces the free surface (135–200 m/s), becomes large ($R_m \approx 45$ μm) relative to the laser spot size and film thickness, and creates a high aspect ratio free-surface jet. For cavities formed at the threshold for jet pinch-off, re-entrant jet formation is suppressed by viscous forces and surface tension. However, larger cavities produced at higher laser energies begin to show evidence of weak re-entrant jets.

Acknowledgments The authors thank Howard Stone, Dmitry Savransky, and Martí Duocastella for valuable discussions in preparing

this manuscript. This work was supported by AFOSR (FA9550-08-1-0094) and NSF (NSF-DMR-0548147). MSB was supported in part by an NSF-IGERT fellowship, Grant #0903661 (Nanotechnology for Clean Energy).

References

Akhatov I, Lindau O, Topolnikov A, Mettin R, Vakhitova N, Lauterborn W (2001) Collapse and rebound of a laser-induced cavitation bubble. Phys Fluids 13(10):2805–2819

Antkowiak A, Bremond N, Le Dizès S, Villermaux E (2007) Short-term dynamics of a density interface following an impact. J Fluid Mech 577:241–250

Arnold CB, Serra P, Piqué A (2007) Laser direct-write techniques for printing of complex materials. MRS Bull 32(1):23–31

Barron JA, Young HD, Dlott DD, Darfler MM, Krizman DB, Ringeisen BR (2005) Printing of protein microarrays via a capillary-free fluid jetting mechanism. Proteomics 5(16):4138–4144

Benjamin TB, Ellis AT (1966) Collapse of cavitation bubbles and pressures thereby produced against solid boundaries. Philos Trans R Soc Lond Ser A 260(1110):221–240

Blake JR, Gibson DC (1987) Cavitation bubbles near boundaries. Annu Rev Fluid Mech 19:99–123

Brown MS, Kattamis NT, Arnold CB (2010) Time-resolved study of polyimide absorption layers for blister-actuated laser-induced forward transfer. J Appl Phys 107(8):083103

Brujan EA, Ohl CD, Lauterborn W, Philipp A (1996) Dynamics of laser-induced cavitation bubbles in polymer solutions. Acustica 82(3):423–430

Brujan EA, Nahen K, Schmidt P, Vogel A (2001) Dynamics of laser-induced cavitation bubbles near an elastic boundary. J Fluid Mech 433:251–281

Calvert P (2001) Inkjet printing for materials and devices. Chem Mater 13(10):3299–3305

Chahine GL, Fruman DH (1979) Dilute polymer solution effects on bubble growth and collapse. Phys Fluids 22(7):1406–1407

Colina M, Duocastella M, Fernández-Pradas JM, Serra P, Morenza JL (2006) Laser-induced forward transfer of liquids: study of the droplet ejection process. J Appl Phys 99(8):084909

Duchemin L, Popinet S, Josserand C, Zaleski S (2002) Jet formation in bubbles bursting at a free surface. Phys Fluids 14(9):3000–3008

Duocastella M, Fernández-Pradas JM, Serra P, Morenza JL (2008) Jet formation in the laser forward transfer of liquids. Appl Phys A 93(2):453–456

Duocastella M, Fernández-Pradas JM, Morenza JL, Serra P (2009) Time-resolved imaging of the laser forward transfer of liquids. J Appl Phys 106(8):084907

Eggers J (1997) Nonlinear dynamics and breakup of free-surface flows. Rev Mod Phys 69(3):865–929

Gekle S, Gordillo JM, van der Meer D, Lohse D (2009) High-speed jet formation after solid object impact. Phys Rev Lett 102(3):034502

Hon KKB, Li L, Hutchings IM (2008) Direct writing technology—advances and developments. CIRP Ann Manuf Technol 57(2):601–620

Kattamis NT, Purnick PE, Weiss R, Arnold CB (2007) Thick film laser induced forward transfer for deposition of thermally and mechanically sensitive materials. Appl Phys Lett 91(17):171120

Kattamis NT, McDaniel ND, Bernhard S, Arnold CB (2009) Laser direct write printing of sensitive and robust light emitting organic molecules. Appl Phys Lett 94(10):103306

Kyrkis KD, Andreadaki AA, Papazoglou DG, Zergioti I (2006) Direct transfer and microprinting of functional materials by laser-induced forward transfer. In: Perriere J, Millon E, Fogarassy E (eds) Recent advances in laser processing of materials. Elsevier, New York, pp 213–241

Lewis BR, Kinzel EC, Laurendeau NM, Lucht RP, Xu X (2006) Planar laser imaging and modeling of matrix-assisted pulsed-laser evaporation direct write in the bubble regime. J Appl Phys 100(3):033107

Liu XM, He J, Lu J, Ni XW (2009) Effect of liquid viscosity on a liquid jet produced by the collapse of a laser-induced bubble near a rigid boundary. Jpn J Appl Phys 48(1):016504

Mézel C, Hallo L, Souquet A, Breil J, Hébert D, Guillemot F (2009) Self-consistent modeling of jet formation process in the nano-second laser pulse regime. Phys Plasmas 16(12):123112

Minsier V, De Wilde J, Proost J (2009) Simulation of the effect of viscosity on jet penetration into a single cavitating bubble. J Appl Phys 106(8):084906

Pearson A, Cox E, Blake JR, Otto SR (2004) Bubble interactions near a free surface. Eng Anal Bound Elem 28(4):295–313

Philipp A, Lauterborn W (1998) Cavitation erosion by single laser-produced bubbles. J Fluid Mech 361:75–116

Piqué A, Chrisey DB, Auyeung RCY, Fitz-Gerald J, Wu HD, McGill RA, Lakeou S, Wu PK, Nguyen V, Duignan M (1999) A novel laser transfer process for direct writing of electronic and sensor materials. Appl Phys A 69:S279–S284

Piqué A, Kim H, Arnold CB (2006) Laser forward transfer of electronic and power generating materials. In: Phipps CR (ed) Laser ablation and applications. Springer, Berlin, pp 339–373

Plesset MS, Chapman RB (1971) Collapse of an initially spherical vapour cavity in neighbourhood of a solid boundary. J Fluid Mech 47:283–290

Popinet S, Zaleski S (2002) Bubble collapse near a solid boundary: a numerical study of the influence of viscosity. J Fluid Mech 464:137–163

Robinson PB, Blake JR, Kodama T, Shima A, Tomita Y (2001) Interaction of cavitation bubbles with a free surface. J Appl Phys 89(12):8225–8237

Serra P, Fernández-Pradas JM, Colina M, Duocastella M, Dominguez J, Morenza JL (2006) Laser-induced forward transfer: a direct-writing technique for biosensors preparation. J Laser Micro/Nanoeng 1(3):236–242

Singh M, Haverinen HM, Dhagat P, Jabbour GE (2010) Inkjet printing—process and its applications. Adv Mater 22(6):673–685

Smausz T, Hopp B, Kecskeméti G, Bor Z (2006) Study on metal microparticle content of the material transferred with absorbing film assisted laser induced forward transfer when using silver absorbing layer. Appl Surf Sci 252(13):4738–4742

Young D, Auyeung RCY, Piqué A, Chrisey DB, Dlott DD (2002) Plume and jetting regimes in a laser based forward transfer process as observed by time-resolved optical microscopy. Appl Surf Sci 197–198:181–187

Yu PW, Ceccio SL, Tryggvason G (1995) The collapse of a cavitation bubble in shear flows—a numerical study. Phys Fluids 7(11):2608–2616

Zeff BW, Kleber B, Fineberg J, Lathrop DP (2000) Singularity dynamics in curvature collapse and jet eruption on a fluid surface. Nature 403(6768):401–404